AD-A171 078 THICK DIELECTRIC CHARGING ON HIGH-ALTITUDE SPACECRAFT 1/1
(U) AEROSPACE CORP EL SEGUNDO CA SPACE SCIENCES LAB
A L VAMPOLA 25 JUL 86 TR-0086(6940-05)-7 SD-TR-86-46
UNCLASSIFIED F04701-85-C-0086 F/G 22/1 NL

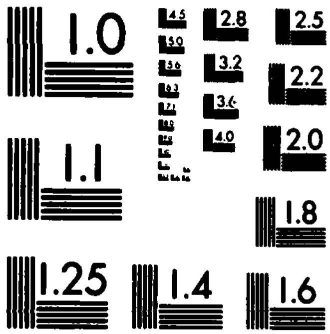
1.0
2.8
2.5
3.2
2.2
3.6
4.0
2.0
1.1
1.8
1.25
1.4
1.6

(12)

REPORT SD-TR-86-46

AD-A171 078

Thick Dielectric Charging on High-Altitude Spacecraft

A. L. VAMPOLA
Space Sciences Laboratory
Laboratory Operations
The Aerospace Corporation
El Segundo, CA 90245

DTIC FILE COPY

25 July 1986

APPROVED FOR PUBLIC RELEASE;
DISTRIBUTION UNLIMITED

Prepared for

SPACE DIVISION
AIR FORCE SYSTEMS COMMAND
Los Angeles Air Force Station
P.O. Box 92960, Worldway Postal Center
Los Angeles, CA 90009-2960

86 061

This report was submitted by The Aerospace Corporation, El Segundo, CA 90245, under Contract No. F04701-85-C-0086 with the Space Division, P.O. Box 92960, Worldway Postal Center, Los Angeles, CA 90009-2960. It was reviewed and approved for The Aerospace Corporation by H. R. Rugge, Director, Space Sciences Laboratory. Capt Douglas R. Case, SD/YCM, was the project officer for the Mission-Oriented Investigation and Experimentation (MOIE) Program.

This report has been reviewed by the Public Affairs Office (PAS) and is releasable to the National Technical Information Service (NTIS). At NTIS, it will be available to the general public, including foreign nationals.

This technical report has been reviewed and is approved for publication. Publication of this report does not constitute Air Force approval of the report's findings or conclusions. It is published only for the exchange and stimulation of ideas.

Douglas R. Case

DOUGLAS R. CASE, Capt, USAF
MOIE Project Officer
SD/YCM

Joseph Hess

JOSEPH HESS, GM-15
Director, AFSTC West Coast Office
AFSTC/WCO OL-AB

ADA171078

UNCLASSIFIED

SECURITY CLASSIFICATION OF THIS PAGE (When Data Entered)

REPORT DOCUMENTATION PAGE

READ INSTRUCTIONS BEFORE COMPLETING FORM

1. REPORT NUMBER SD-TR-86-46	2. GOVT ACCESSION NO.	3. RECIPIENT'S CATALOG NUMBER
4. TITLE (and Subtitle) THICK DIELECTRIC CHARGING ON HIGH-ALTITUDE SPACECRAFT		5. TYPE OF REPORT & PERIOD COVERED
		6. PERFORMING ORG. REPORT NUMBER TR-0086(6940-05)-7
7. AUTHOR(s) Alfred L. Vampola		8. CONTRACT OR GRANT NUMBER(s) F04701-85-C-0086
9. PERFORMING ORGANIZATION NAME AND ADDRESS The Aerospace Corporation El Segundo, Calif. 90245		10. PROGRAM ELEMENT, PROJECT, TASK AREA & WORK UNIT NUMBERS
11. CONTROLLING OFFICE NAME AND ADDRESS Space Division Los Angeles Air Force Station Los Angeles, Calif. 90009-2960		12. REPORT DATE 25 July 1986
		13. NUMBER OF PAGES 21
14. MONITORING AGENCY NAME & ADDRESS(if different from Controlling Office)		15. SECURITY CLASS. (of this report) Unclassified
		15a. DECLASSIFICATION/DOWNGRADING SCHEDULE

16. DISTRIBUTION STATEMENT (of this Report)

Approved for public release; distribution unlimited.

17. DISTRIBUTION STATEMENT (of the abstract entered in Block 20, if different from Report)

18. SUPPLEMENTARY NOTES

19. KEY WORDS (Continue on reverse side if necessary and identify by block number)

Spacecraft anomalies
Spacecraft charging
Magnetospheric environment
Van Allen electrons

20. ABSTRACT (Continue on reverse side if necessary and identify by block number)

Thick dielectric charging, in which energetic electrons embed within bulk dielectrics and build up to potentials in excess of the breakdown potential of the dielectric, is shown to be a causative factor in the anomalous operation of high-altitude satellites. Results of laboratory studies are reviewed and a table of maximum expected electron fluxes in orbits of various altitude is presented. The combination of maximum expected electron fluxes and the small energy associated with a bulk dielectric breakdown permits the elimination of bulk charging as a spacecraft problem through the

DD FORM 1473 FACSIMILE

UNCLASSIFIED

SECURITY CLASSIFICATION OF THIS PAGE (When Data Entered)

19. KEY WORDS (Continued)

20. ABSTRACT (Continued)

minimal shielding (400 mg/cm^2) of all cables and circuit boards otherwise exposed to the environment, and through the desensitizing of digital logic inputs that are serviced by cables.

PREFACE

The author wishes to express his gratitude to Dom Scrooc, who first brought the thick dielectric charging mechanism to his attention; to members of the Space Environment Laboratory, NOAA, who provided GOES high-energy electron data for anomaly analyses; and to Drs. J. Fennell, R. Nightingale, and P. Robinson, who provided the results of analyses used in this study.

CONTENTS

FIGURES

TABLES

I. INTRODUCTION

The problem of electrostatic discharge on satellites as a result of the environment in which they operate has received much attention since it was first recognized on the ATS-5 satellite in 1970.[1] A series of conferences was devoted to the subject[2,3,4,5] and the SCATHA program[6] was specifically directed to study thoroughly the mechanisms associated with spacecraft charging, its causes, and its amelioration. The results of that program, which included an instrumented spacecraft flown in the geosynchronous region,[7] are now being applied to the design of spacecraft.[8,9] The major thrust of spacecraft charging studies has been directed toward the surface charging of dielectrics in the presence of hot plasmas.

However, a second electrostatic charging mechanism was postulated[10] in which incident high-energy electrons embed within the bulk of a thick dielectric, such as in a cable or a circuit board, and build up a potential. If a secondary electron is emitted from the surface by the incident electron, the net charge of the dielectric may remain low, or zero, but a large field may build up in the dielectric. Wenaas[11] and Beers[12] calculated the conditions that would exist within a thick dielectric that is irradiated with energetic electrons. The resulting potential is a function of the geometry, flux, and energy spectrum of the incident electrons, and of the conductivity of the dielectric. If the rate of charge deposition resulting from the incident flux exceeds the rate at which charge leaks out as a result of the conductivity of the material, as enhanced by radiation-induced conductivity caused by the incident flux itself, the potential in the bulk dielectric can exceed the breakdown potential for that material, resulting in a discharge.

Experimental results from electron beam irradiation of various dielectrics have shown[13] that breakdown does occur as predicted at a typical integrated fluence of 10^{12} e^-/cm^2. Other studies have parameterized the response of typical circuit board[14] and cable[15] dielectrics. In a typical thick dielectric discharge, a very small portion of the dielectric is involved. The maximum discharge measured by Wenaas et al.[14] was 4 μJ in 50 ohms. A pulse

this size and smaller would normally be considered to be a spurious signal, although there is sufficient energy to damage some semiconductor junctions or particularly sensitive devices. Currents measured in cable discharges were of the order of amperes in the shield and tens of milliamperes in the center conductor.[15] All pulses were in the tens of nsec range.

The mechanism has been established in the laboratory, but two questions remain to be answered: (1) is the energetic electron population in space ever sufficiently intense to produce such discharges, and (2) to what extent do spacecraft actually experience thick dielectric discharges? We will address these two questions in the next two sections.

II. THE PEAK ENERGETIC ELECTRON FLUX

A search of published and unpublished data was made to identify the maximum flux that could be expected in the outer zone as a result of naturally occurring electrons. The unpublished data included results from OGO-5,* OV3-3, and OV1-19. The period included data from 1964 to 1975, which encompasses a complete solar cycle and should probably represent a typical solar cycle. Data from OV3-3 and OV1-19 were obtained at relatively low altitude (4500 to 5000 km) and were extrapolated back to the equatorial region by means of equatorial pitch-angle distribution functions available from the OGO-5 data set. The OGO-5, OV3-3, and OV1-19 data were available as unidirectional, differential flux (units of e^-/cm^2-sec-ster-keV) at various energies and L-values. L is McIlwain's parameter[16] and in a dipole field corresponds to the radial distance from the center of the dipole to the equatorial crossing of the magnetic field line in units of earth-radii. The other data sets, from Explorer 14, ATS-1, and OGO-1 and OGO-3, present their results as integral omnidirectional fluxes (units of e^-/cm^2-sec above a threshold).

To combine the results of the two tables, one must integrate the energy spectra presented in Table 1 to get integral spectra above a threshold, and then convert unidirectional flux to omnidirectional flux (Table 2). For the electron pitch-angle distributions present in the outer zone, a reasonable conversion is to multiply the unidirectional flux by 3.5π. For the purposes of calculating the susceptibility of spacecraft to thick dielectric charging, the peak fluxes in Table 3 are recommended.

Note that this last table gives integral-omnidirectional peak flux above the threshold energies shown. In all cases, fluxes in space have been observed to get within a factor of 2 of these figures. For a wider range of energy and spatial location, one can get an estimate of the peak flux by calculating the peak stable flux predicted by the Kennel-Petschek theory[17] and multiplying by a factor of 10. A complete relativistic treatment of flux limiting produces a stable limit that is about a factor of 2 higher than

*H. I. West, Jr., private communication.

Table 1. Maximum Unidirectional Electron Fluxes

Satellite	Energy, keV	L=4.0	L=4.5	L=5.0	L=5.5	L=6.0
OGO-5	266	1.5×10^4	8×10^3	4.5×10^3		3.5×10^3
	478	6×10^3	6×10^3	3×10^3		1.5×10^3
	822	2.5×10^4	1.8×10^4	1×10^4		5×10^3
	1530	1.8×10^4	1.1×10^4	5×10^3		1.8×10^4
	2830	1.5×10^3	8×10^2	4×10^2		7×10^1
OV3-3	300	2.5×10^4				
	712	2.5×10^4				
	1220	5×10^3				
OV1-19	540		4×10^3		2×10^4	
	2600		4×10^3		8×10^2	
	5100		6×10^2		1×10^2	

Table 2. Maximum Omnidirectional Electron Fluxes

Satellite	Energy, MeV	L=4.0	L=4.5	L=5.0	L=6.6
EXP-14	0.5	8×10^7		6×10^7	
	1.6	5×10^5		7×10^5	
OGO-1, -3	2.0		5×10^5	2×10^6	2×10^5
ATS-1	0.32				3×10^7
	1.0				2×10^5

Table 3. Peak Recommended Electron Fluxes

Energy, MeV	L=4.0	L=4.5	L=5.0	L=5.5	L=6.0	L=6.6
0.5	6×10^8	4×10^8	2×10^8	1.5×10^8	1×10^8	5×10^7
1.0	1×10^8	6×10^7	3×10^7	2×10^7	1×10^7	5×10^6
2.0	4×10^6	2×10^6	1×10^6	7×10^5	5×10^5	2×10^5

that resulting from the nonrelativistic treatment of Ref. 17. For the purposes of computing rate effects in thick dielectrics, one should assume that these peak fluxes are present for about one day. Fluxes can exceed the Kennel-Petschek limit for several days. One can see that unprotected dielectrics can experience a total fluence of 10^{12} e^{-}/cm^{2} in one to several hours when in an environment as severe as those of Table 3.

III. THICK DIELECTRIC CHARGING IN SPACE

Beginning in 1977, analyses of the anomalous behavior of Air Force satellites implicated the energetic electron environment in a number of instances. In the first case, a spurious signal in an exposed power-control cable appeared to be the cause of a subsystem failure. The satellite did not carry environmental sensors, but data from other satellites indicated that surface-charging conditions (hot plasma with a very low-density cold plasma) were probably not present, although a markedly enhanced energetic electron flux was present. The tentative diagnosis was that failure resulted from electrostatic discharge caused by thick dielectric charging in the exposed cable.

When the NTS-2 satellite, a demonstration satellite for the Global Positioning System program, was launched in 1978, a series of clock anomalies occurred which were correlated with a large magnetic storm that had accelerated high fluxes of energetic electrons in the outer magnetosphere. Again, surface charging was eliminated as a potential cause and a tentative identification of thick dielectric charging was made.* Fluxes of the order of 10^{12} e^-/cm^2-day were estimated from dosimeter data aboard NTS-2. Spurious pulses in a cable irradiated by the energetic electrons were thought to be causing a bit shift in a tuning register.

The above examples were not amenable to verification of the hypothesized causes of the anomalies. When Voyager 1 encountered Jupiter on 5 March 1979, a series of Power on Reset (POR) anomalies occurred just prior to and during a critical photographic sequence at the closest approach to the planet. Because of the long propagation delay (about an hour) for signals to Voyager 1 at that distance, instructions for photo sequences were loaded into an on-board memory and an on-board clock was used to time the actual operation. As part of the power system, a logic signal was used to initialize critical functions whenever the power was momentarily disrupted. The POR itself inhibited the on-board clock, causing a cumulative offset in the clock each time a POR occurred. Figure 1 shows the cumulative sequence of PORs during the encounter

*J. B. Blake, private communication.

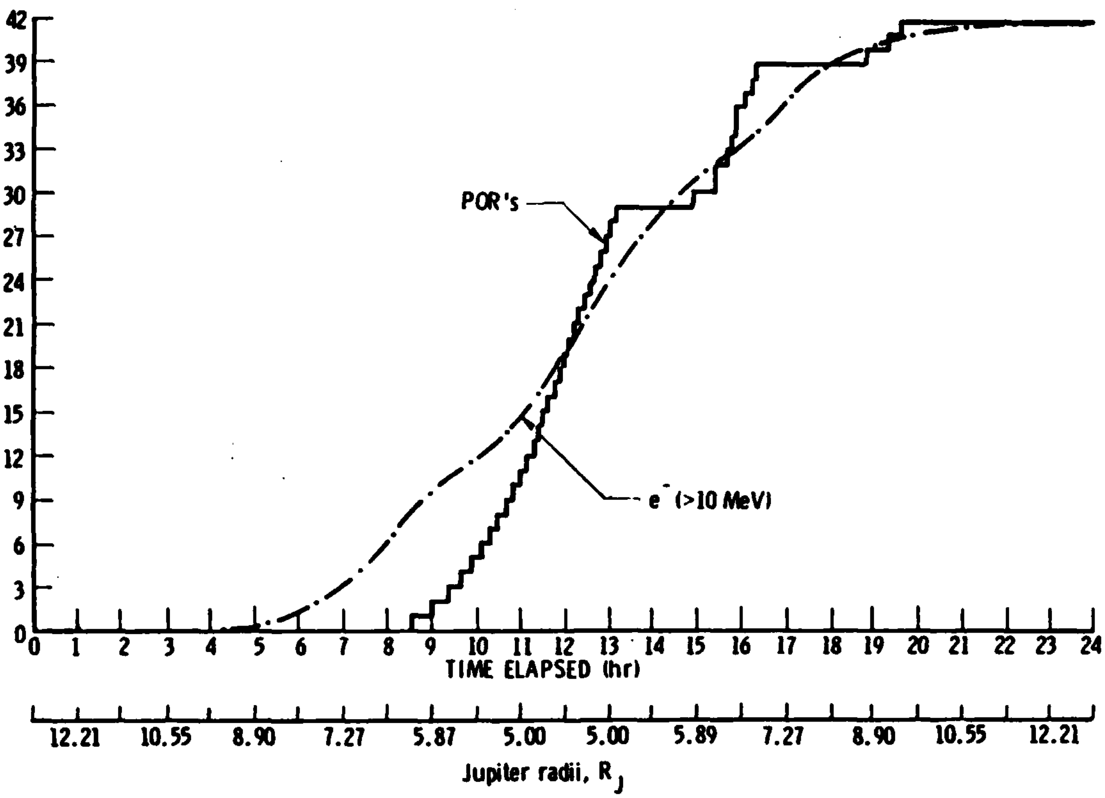

Fig. 1. Voyager-1 Power On Reset Anomalies During Jupiter Encounter

period.* An investigation into the cause of the anomalies showed that the POR signal was normally carried in a cable from the box in which it was generated and back to the same box, where it was utilized. The POR cable was part of a cable bundle that included unterminated spares; this bundle exited the spacecraft and then reentered. Testing of a mockup in the laboratory showed that small (25 ma) pulses in wires in the cable bundle would couple into the POR cable and cause a spurious POR response.

Since the cold plasma density, as measured by on-board instruments, around the spacecraft during most of this period was too high to permit surface charging in excess of a few volts, other components of the environment were investigated. The only component that showed a similar encounter profile was the measurement of electrons with energy in excess of 10 MeV. The cumulative fluence of these electrons is also plotted in Fig. 1. The evidence supported a conclusion that thick dielectric charging was the cause of the POR anomalies.

An exhaustive investigation of a large number of anomalies observed on METEOSAT-1 resulted in the conclusion that surface charging was occurring, along with surface discharges (though these did not cause most of the anomalies), and also that the only geophysical parameter that correlated with the anomalies was the occurrence of magnetic storms.[18] The anomalies were occurring one to several days after the storms, not during them as would have been the case if hot plasma induced surface charging. The increase in energetic electrons at synchronous orbit altitudes also shows a delay of one to several days after large magnetic storms. Modifications to METEOSAT-2 included desensitizing circuits to small spurious pulses. The vehicle was much less subject to anomalies than its predecessor.[19]

Another program, the Air Force Defense Support Program, experienced anomalies that were strongly correlated with the energetic electron fluxes in this environment. Although vehicles had been on orbit for a number of years following the solar sunspot maximum of 1969, the first star-sensor shutter anomaly occurred in 1976, following a magnetic storm. A second one occurred in 1978. Then, during the magnetically active period from 1980 to 1982, a

*P. Robinson, private communication.

series of them occurred. Figure 2 shows the energetic electron flux at geosynchronous orbit as measured by GEOS-2 for a 2-yr. period. The time of shutter anomalies is shown by arrows. The correlation of anomalies with energetic electron fluxes is unambiguous. The vehicles involved have a sun sensor mounted on a shade that protects the star sensor. A signal in the sun sensor closes the shutter to prevent exposure of the star sensor to the full intensity of sunlight. A cable connecting the sun sensor to control electronics in the vehicle exits the vehicle and is routed to the sun sensor along the shade. The probable cause of these anomalies was spurious pulses in the unprotected cable as a result of discharges in the dielectric in the cable. The discharges were caused by imbedded charge that in turn was the result of the enhanced energetic electron fluxes.

A final example of an anomaly caused by thick dielectric discharges is evaluated in Fig. 3. In this case the vehicle involved was the GPS satellite and the anomaly was an uncommanded switch from autotrack to manual mode of the solar panel orientation system. Again, a spurious signal in an unshielded cable was the probable immediate cause. Data from another satellite in the vicinity, SCATHA, indicated that surface charging could not have been the cause but that a very high energetic electron flux was present (the highest that had been observed by SCATHA in its 16 months on orbit).* Within an hour of the time that the GPS anomaly occurred, SCATHA, which was located at approximately the same altitude and local time, had its first environmentally induced anomaly, an uncommanded mode change in its magnetometer. The magnetometer control cable is exposed in its 7-m run along a boom.

Figure 3 presents electron fluxes as a function of energy for a number of different elements. The circles are the maximum fluxes expected in the GPS orbit, derived from Table 3. "C" refers to results from tests of cables[15] and "B" refers to circuit board tests[14] that produced discharges. The squares are the actual fluxes measured by the SC3 electron spectrometer on SCATHA at the time of the anomaly.* In the GPS anomaly, as in most anomaly investigations in which thick dielectric charging is implicated, a spurious pulse occurring in an exposed cable could have produced the symptoms observed; no other plausible mechanism was identified.

*R. Nightingale, private communication.

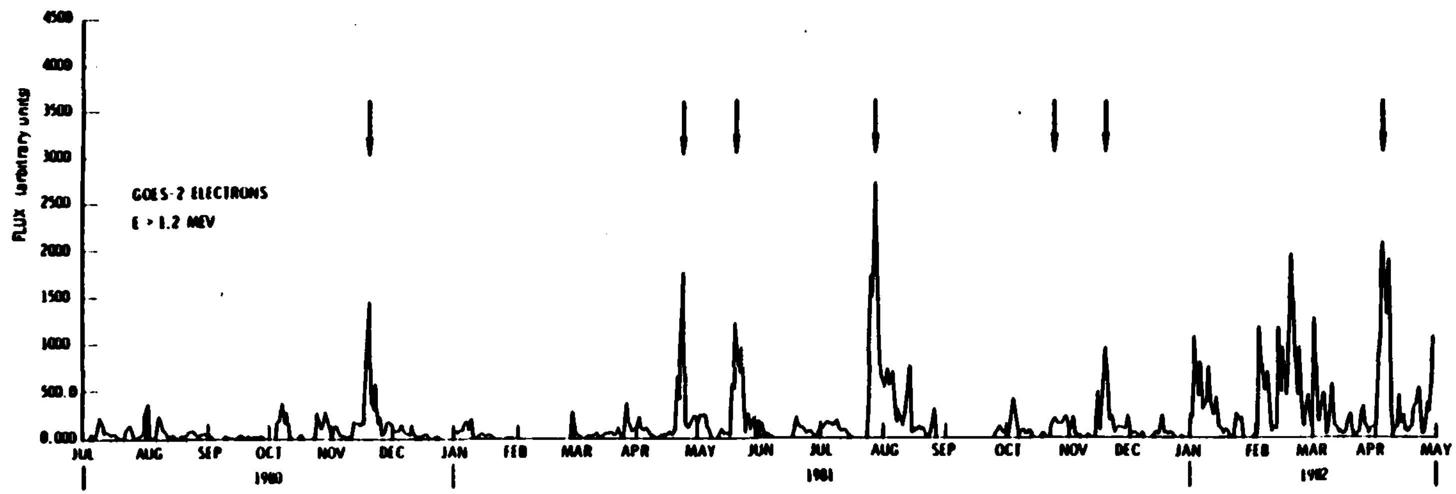

Fig. 2. DSP Star Sensor Anomalies and GOES-2 Electron Flux

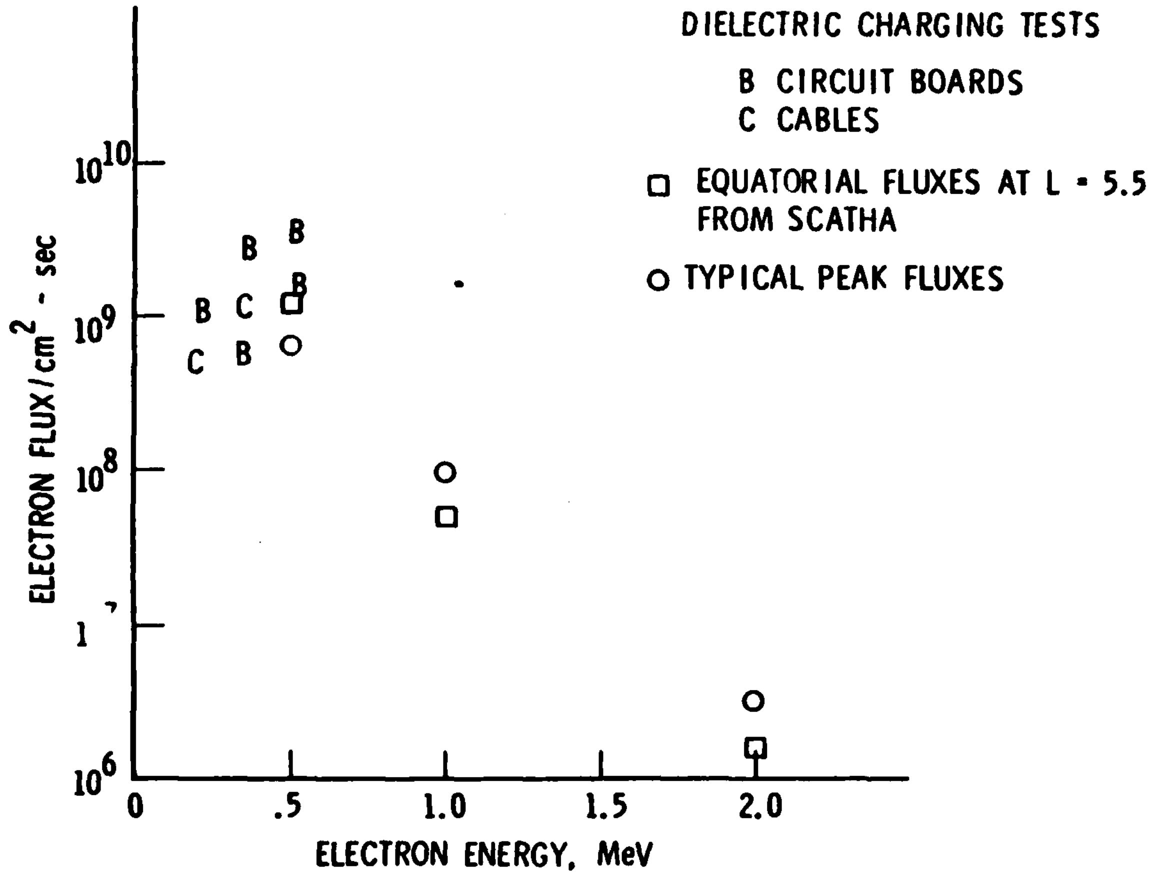

Fig. 3. Electron Fluxes vs. Energy for Thick Dielectric Discharges

Thus far, data concerning thick dielectric charging anomalies on operational spacecraft are difficult to elicit and usually appear in anecdotal form. Thus, it is difficult to determine the relative frequency of such anomalies, especially as compared to anomalies produced by surface-charging conditions. However, it is possible to make an educated guess as to the relative importance of this mechanism compared to that of surface charging. Figure 4 presents a summary of anomalies on a number of spacecraft which were thought to have been caused by electrostatic discharge.* The plot only shows the local time of the anomaly (bracketed by a bar when the precise time could not be determined). This plot predates the awareness and investigation of thick dielectric charging. It is useful to note that the thick dielectric charging mechanism is independent of local time. At the same time, surface charging to high potentials is a strong function of local time,[20] being confined to the local time sector from premidnight to dawn.

If we assume that thick dielectric charging has an equal probability of occurring at any local time, we can estimate the portion of the anomalies charted in Fig. 4 that were due to thick dielectric charging. No surface charging should be observed in the prenoon (10:00) to dusk (20:00) sector. If we ascribe all of these anomalies to thick dielectric charging and extrapolate to a 24-hr. period, we find that almost exactly half of the anomalies were due to thick dielectric charging. That is a rather surprising result, considering the vast amount of attention that surface charging has gotten through the years and the lack of interest shown in thick dielectric charging. On the other hand, thick dielectric charging is much more easily dealt with than surface charging, and so perhaps deserved less attention.

*J. F. Fennell, private communication.

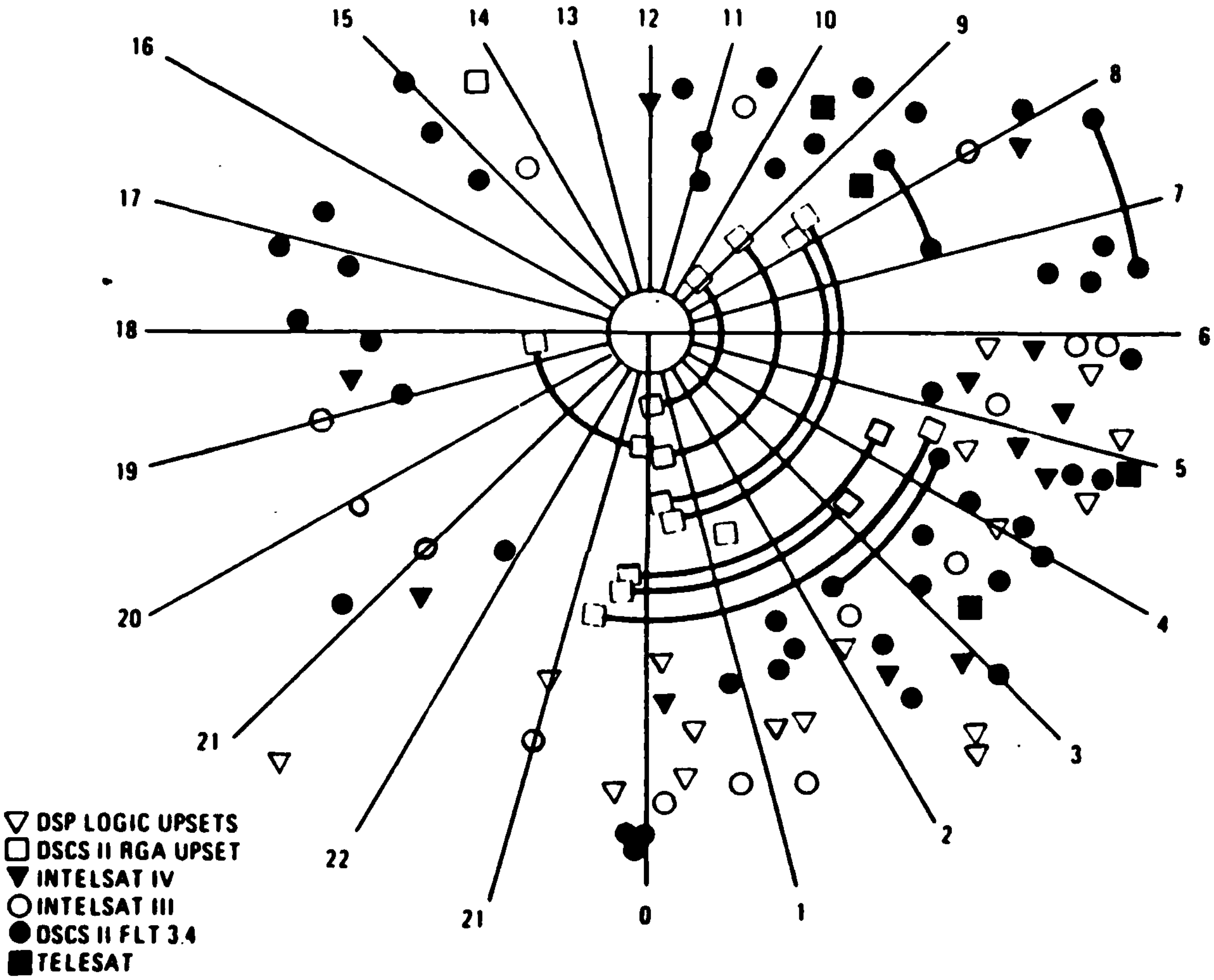

Fig. 4. Local-Time Plot of Anomalies on Operational Spacecraft

IV. DISCUSSION AND SUMMARY

Thick dielectric charging has been shown both theoretically and experimentally in the laboratory to be a potentially disrupting mechanism on satellites. Since the causative agent, high-energy electrons, can be found at times throughout the magnetosphere, this hazard is of concern to all spacecraft, not just to those that operate in the near-synchronous region (where the surface charging mechanism is operative). On the other hand, it is trivially simple to prevent this mechanism from causing discharges in sensitive circuits or producing false command pulses. The total fluence required to produce sufficient charge buildup to produce a discharge is of the order of 10^{12} e^-/cm^2 in a period that is short compared to the charge bleedoff time of the dielectric. Typically, fluxes low enough that more than a few hours are required to produce this fluence will not normally produce discharges. Thus, a lower limit of a few times 10^8 e^-/cm^2-sec at the surface of the dielectric is required. From Table 3 it can be determined that shielding that eliminates all electrons with energies below 1 MeV should prevent thick dielectric discharges. This is equivalent to 60 mil of Al. Since circuit boards are normally enclosed within boxes that are in turn enclosed within the satellite, it is unlikely that special precautions need be taken for circuit boards. The self-shielding resulting from metal cladding and components also assists in preventing significant charge buildup. However, exposed cables can be (and have been) troublesome.

For cables exposed to the environment, the following solutions are readily available: (1) Don't expose them to the environment. (2) If they have to be placed outside the body of the spacecraft, shield them. (3) All digital circuits that derive an input signal from a cable coming into the box in which the circuit is located should be designed to survive and not respond to signals of the type generated in thick dielectric discharges. Satellites designed with SGEMP protection will probably not be affected by static discharges, whether such discharges are caused by surface or thick dielectric charging.

REFERENCES

1. DeForest, S. E., Spacecraft Charging at Synchronous Orbits, J. Geophys. Res. 77, 1972, pp. 651-659.

2. Spacecraft Charging by Magnetospheric Plasmas, AIAA Progress in Astronautics and Aeronautics, Vol. 47, A. Rosen, ed., 1976.

3. Proceedings of the Spacecraft Charging Technology Conference, NASA TMX-73537, 1977.

4. Spacecraft Charging Technology-1978, NASA CP 2071, 1979.

5. Spacecraft Charging Technology-1980, NASA CP 2182, 1981.

6. McPherson, D. A. and W. R. Schober, Spacecraft Charging at High Altitudes: The SCATHA Satellite Program, in Spacecraft Charging by Magnetospheric Plasmas, AIAA Progress Series, Vol. 47, A. Rosen, ed., 1976, pp. 15-30.

7. Journal of Spacecraft and Rockets, Special SCATHA Section, Vol. 20, No. 5, 1983, pp. 417-449.

8. Design Guidelines for Assessing and Controlling Spacecraft Charging Effects, NASA TP 2361, 1984.

9. The Aerospace Spacecraft Charging Document, SD TR-0084A(5940-05)-10, 1985.

10. Meulenberg, A., Jr., Evidence for a New Discharge Mechanism for Dielectrics in a Plasma, in Spacecraft Charging by Magnetospheric Plasmas, AIAA Progress Series, Vol. 47, A. Rosen, ed., 1976, pp. 237-246.

11. Wenaas, E. P., Spacecraft Charging Effects by the High-Energy Natural Environment, IEEE Trans. Nuc. Sci. NS-24, 1977, pp. 2281-2284.

12. Beers, B. L., Radiation-Induced Signals in Cables-II, IEEE Trans. Nuc. Sci. NS-24, 1977, pp. 2429-2434.

13. Frederickson, A. R., Bulk Charging and Breakdown in Electron-Irradiated Polymers, in Spacecraft Charging Technology-1980, NASA CP 2192, 1981, pp. 33-51.

14. Wenaas, E. P., M. J. Treadaway, T. M. Flanagan, C. E. Mallon, and R. Denson, High-Energy Electron-Induced Discharges in Printed Circuit Boards, IEEE Trans. Nuc. Sci., NS-26, 1979, pp. 5152-5155.

15. Mallon, C. E., M. J. Treadaway, T. M. Flanagan, E. P. Wenaas, and R. Denson, High-Energy Electron-Induced Discharges and SGEMP Modification in Cables, AFWL ECEMP Phenomenology Memo No. 29, 1979.

16. McIlwain, C. E., Coordinates for Mapping the Distribution of Magnetically-Trapped Particles, J. Geophys. Res. 66, 1961, pp. 3681-3691.

17. Kennel, C. F., and H. E. Petschek, Limit on Stably Trapped Particle Fluxes, J. Geophys. Res. 71, 1966, pp. 1-28.

18. Robbins, A., METEOSAT Spacecraft Charging Investigation, European Space Agency Report ESA CR(X) 1346, 1979.

19. Johnstone, A. D., G. L. Wrenn, A. Huber, and D. Hoge, First Results from METEOSAT-2 Discharge Experiments, ESA Bulletin 29, 1982, pp. 84-89.

20. Mizera, P. F., and G. Boyd, A Summary of Spacecraft Charging Results, J. Spacecraft and Rockets 20, 1983, pp. 438-443.

LABORATORY OPERATIONS

The Aerospace Corporation functions as an "architect-engineer" for national security projects, specializing in advanced military space systems. Providing research support, the corporation's Laboratory Operations conducts experimental and theoretical investigations that focus on the application of scientific and technical advances to such systems. Vital to the success of these investigations is the technical staff's wide-ranging expertise and its ability to stay current with new developments. This expertise is enhanced by a research program aimed at dealing with the many problems associated with rapidly evolving space systems. Contributing their capabilities to the research effort are these individual laboratories:

Aerophysics Laboratory: Launch vehicle and reentry fluid mechanics, heat transfer and flight dynamics; chemical and electric propulsion, propellant chemistry, chemical dynamics, environmental chemistry, trace detection; spacecraft structural mechanics, contamination, thermal and structural control; high temperature thermomechanics, gas kinetics and radiation; cw and pulsed chemical and excimer laser development including chemical kinetics, spectroscopy, optical resonators, beam control, atmospheric propagation, laser effects and countermeasures.

Chemistry and Physics Laboratory: Atmospheric chemical reactions, atmospheric optics, light scattering, state-specific chemical reactions and radiative signatures of missile plumes, sensor out-of-field-of-view rejection, applied laser spectroscopy, laser chemistry, laser optoelectronics, solar cell physics, battery electrochemistry, space vacuum and radiation effects on materials, lubrication and surface phenomena, thermionic emission, photosensitive materials and detectors, atomic frequency standards, and environmental chemistry.

Computer Science Laboratory: Program verification, program translation, performance-sensitive system design, distributed architectures for spaceborne computers, fault-tolerant computer systems, artificial intelligence, microelectronics applications, communication protocols, and computer security.

Electronics Research Laboratory: Microelectronics, solid-state device physics, compound semiconductors, radiation hardening; electro-optics, quantum electronics, solid-state lasers, optical propagation and communications; microwave semiconductor devices, microwave/millimeter wave measurements, diagnostics and radiometry, microwave/millimeter wave thermionic devices; atomic time and frequency standards; antennas, rf systems, electromagnetic propagation phenomena, space communication systems.

Materials Sciences Laboratory: Development of new materials: metals, alloys, ceramics, polymers and their composites, and new forms of carbon; nondestructive evaluation, component failure analysis and reliability; fracture mechanics and stress corrosion; analysis and evaluation of materials at cryogenic and elevated temperatures as well as in space and enemy-induced environments.

Space Sciences Laboratory: Magnetospheric, auroral and cosmic ray physics, wave-particle interactions, magnetospheric plasma waves; atmospheric and ionospheric physics, density and composition of the upper atmosphere, remote sensing using atmospheric radiation; solar physics, infrared astronomy, infrared signature analysis; effects of solar activity, magnetic storms and nuclear explosions on the earth's atmosphere, ionosphere and magnetosphere; effects of electromagnetic and particulate radiations on space systems; space instrumentation.

END
DTIC
9-86